Plane Waves, Spherical Waves and Angle-dependent P-Wave Reflectivity in Elastic VTI-Models

Arnim B. Haase - Geo-X Systems Ltd.

CSEG Geophysics 2002

Summary:
The AVA-response of VTI-models for AVO-Classes 1 to 4 and two special cases is computed utilizing plane-wave reflection coefficients and the Weyl-integral. It is found that below 30° of angle, in most cases, the spherical VTI-response departs more from an isotropic plane-wave comparison than isotropic spherical responses. Depth dependence of isotropic spherical responses is strongest near critical angles, exactly where important information resides. VTI-type anisotropy shifts this point of maximum sensitivity towards larger angles.

Introduction:
AVO-analysis/inversion is routinely based on linearized approximations to true plane-wave reflection coefficients. These linearized equations trade full Zoeppritz complexity for limited angle range validity. The quest for inversion stability and accuracy has inspired several authors to go beyond linearized approximations in recent years. Three parameter AVO inversion is investigated by Downton and Lines (2001) as well as by Kelly and Skidmore (2001). Lavaud et al. (1999) and Roberts (2000) point out the importance of information near the critical angle and utilize the exact Zoeppritz equations. First order approximations to the full Zoeppritz equations are not only limited to angles of incidence well below critical but also to small changes in elastic properties across the interface (Roberts, 2000), limitations that do not exist for the exact Zoeppritz equations. However, even "exact Zoeppritz" is valid only for plane waves impinging on a plane boundary between isotropic elastic materials in welded contact. Skidmore et al. (2001) report AVO-rollover (diminishing of long offset amplitudes for an otherwise Class 3 AVO anomaly) in Gulf of Mexico data and explain this effect with the aid of anisotropic fluid modelling. The physics of the real earth are more complicated and do not just include anisotropy but also anelasticity. Interfaces between rock-formations are not always (hardly ever?) planar and plane waves are just a mathematical concept. AVO-responses are influenced by thin-bed tuning, by scattering and by converted waves. Even the "welded contact" assumption could sometimes be called into question.

The purpose of this modelling study is to go "beyond Zoeppritz" on two fronts: firstly, the effect of VTI-type anisotropy is included into the equation for angle-dependent P-wave reflectivity and, secondly, wavefronts are assumed to be spherical rather than planar.

Theory:
Plane-wave particle amplitude reflection and transmission coefficients for VTI-media in welded contact, parameterized as a function of horizontal slowness p (the ray parameter), are presented by Graebner (1992) and in refined form by Rueger (1996). These Graebner equations reduce to the well known Zoeppritz equations when the parameters of anisotropy (ϵ, δ and ?) are set to zero. According to Rueger (1996), reflection and transmission in anisotropic media was first discussed by Henneke (1972). Reflection of spherical seismic waves in elastic layered media is investigated by Krail and Brysk (1983). They state that, for reflections from reasonably shallow interfaces, it is necessary to treat the incident wave as spherical rather than plane. This modelling study sheds some light on the question, "How shallow is reasonably shallow?". Krail and Brysk (1983) derive spherical correction factors for the Zoeppritz equations. Many authors have dealt with the fundamental problem of determining the response of a spherical point source from a planar elastic boundary. The formalism for expressing spherical wave fronts as contour integrals over plane waves goes back to Weyl (1919). Here, the formula for generalized PP-reflections from an elastic interface given by Aki and Richards (1980, page 217) is adopted:

$$f = Ai\,w\,e^{-iwt}\int_{0}^{\infty} R_{pp}\,\frac{p}{x}\,J_{0}(wpr)\,e^{iwx\,(z+h)}\,dp$$

where J_{o} is the zeroth order Bessel function,

R_{pp} is the plane P-wave reflection coefficient,

? is the vertical slowness and

p is the horizontal slowness (ray parameter).

For isotropic media, vertical slowness ? and horizontal slowness p are simply related by

$?^2 + p^2 = 1 / a^2$

where a is P-wave velocity.

A more complicated set of equations relating ? to p for the VTI case is given by Graebner (1992) and Rueger (1996).

Modelling:
The two layer models utilized in this study are adapted from an actual gas-sand reservoir in west-central Saskatchewan. Depth to reservoir is 500m and the corresponding two-way travel-time is approximately 500ms which dictates a_1=2000m/sec., and $?_1$ is 2400kg/m³ for the layer just above the reservoir. Layer parameters for AVO-Classes 1 to 3 are derived from Rutherford and Williams (1989), and Class 4 values are calculated from the example given by Castagna et al. (1998). Table 1 shows the layer parameters for all classes. Also included are two special cases (Bill Goodway, personal communication): Class 1f is a false AVO anomaly, the PP-reflection coefficient is strongly positive and

amplitudes are decreasing with offset below 30° of angle (mirror image of CLass 4), but this is not a hydrocarbon indicator. Class 3/4 is the boundary between Classes 3 and 4 where the two-term approximation AVO-gradient is zero, meaning there is no amplitude variation with offset (the amplitude is constant) but there could be hydrocarbons.

Class	1	1f	2	3	4	3/4
a_1/[m/s]	2000	2000	2000	2000	2000	2000
β_1/[m/s]	879.9	1000	879.9	879.9	1000	1000
ρ_1/[kg/m³]	2400	2400	2400	2400	2400	2400
a_2/[m/s]	2933	2933	2400	1964	1599	1636
β_2/[m/s]	1882	1453	1540	1260	654.3	904.8
ρ_2/[kg/m³]	2000	2000	2000	2000	2456	2400

Table 1

A 5/15-80/100 Hz Ormsby wavelet is used for the computations. Numerical experiments with different high-frequency and low-frequency roll-offs resulted in only small changes of the computed particle amplitude reflection coefficients (not shown in this abstract). All computations assume circular wavefronts (emanating from a point source) and free surface effects are not considered. The resulting reflection amplitudes are normalized to zero offset plane wave reflection coefficients, no other spreading compensation is applied. Figs. 1 to 6 show spherical-wave results for the six AVO-Classes of Table 1 at depths of 500m, 1000m and 2000m and assuming isotropy in both layers. Also displayed for all AVO-Classes are an isotropic plane wave comparison and a VTI-anisotropic spherical wave example for 500m depth (weak first layer anisotropy with $e_1=0.15$ and $d_1=0.05$). The poster will show more plane-wave comparisons and also examples for moderate as well as strong anisotropy. Except for Fig. 2 (Class 1f), the diagrams are all plotted at the same scale. It should be noted that reflection coefficient magnitude is displayed in all Figures in this abstract.

Discussion and Conclusions:

A cursory inspection of the displays shows two main AVA-response groups. Even though there is a difference between spherical-wave and plane-wave responses for Classes 3 (Fig.4), 4 (Fig.5) and 3/4 (Fig.6), the basic shape of the spherical-wave response is independent of depth because of the zero-offset plane-wave R_{pp} normalization (there is a 1/z scaling difference without normalization). Classes 3, 4 and 3/4 have strongly negative zero-offset reflection coefficients because of a P-wave velocity inversion (see Table 1), head-waves are not generated since there is no critical angle. From Table 1 it is clear that for Classes 1 (Fig.1), 1f (Fig.2) and 2 (Fig.3) P-wave velocities are increasing across the interface, critical angles exist and head-waves are generated. Near and beyond critical angles head-waves contribute to the total AVA-response and cause depth dependence of spherical waves. The Class 1 response in Fig.1 starts with a strongly positive R_{pp} at zero-offset, crosses over to negative R_{pp} at about 27° and then returns to positive R_{pp} near the critical angle just above 40°. There is very little difference between spherical-wave and plane-wave response below 30°. As expected, the larger the curvature radius of spherical waves, the closer the AVA-response to the plane-wave comparison. Weak VTI-type anisotropy causes an apparent shift away from the plane-wave response toward smaller depth. There are significant differences in the VTI-curve even below 30°: the AVA-gradient is reduced. The Class 1f response in Fig.2 is always positive but there is a negative AVA-gradient below about 25°. Plane-wave and spherical-wave responses differ beyond 20°. Depth dependence for spherical waves becomes noticeable beyond 35° and, as before, a larger curvature radius moves AVA-responses closer to the plane-wave comparison. Also as before, the weak VTI-response is shifted away from the plane-wave response, but the AVA-gradient is increased beyond 15°, pushing closer to a true Class 1 response. Below 25° VTI-type anisotropy is narrowing the gap between true and false Class 1. Class 2 responses (Fig.3) have small zero-offset reflection coefficients (positive or negative) and negative AVA-gradients. The gradient changes polarity beyond 30° and R_{pp} changes polarity near the critical angle, not unlike a true Class 1 response at larger angles (around 55° in the example of Fig.3). Also like true Class 1 responses, a larger curvature radius pushes this Class 2 response closer to the plane-wave comparison and weak VTI-type anisotropy moves it away, the negative AVA-gradient is reduced beyond 15° up to about 45°. Spherical-wave and plane-wave response are different below 30° (down to about 23°) and the spherical-wave depth dependence becomes significant beyond 50°. Classes 3, 4 and 3/4 have strong negative zero-offset reflection coefficients, spherical-wave and plane-wave responses differ beyond about 20°. Class 3 (Fig.4) has a negative AVA-gradient which is decreased by anisotropy below 40°. Class 4 (Fig.5) shows a positive AVA-gradient which is also decreased by anisotropy below 45°, the spherical-wave response is close to the plane-wave response out to about 50°. Class 3/4 (Fig.6) is essentially flat below 25° (zero AVA-gradient). The VTI-response and even more so the spherical-wave response remain quite flat all the way out beyond 70° while the plane-wave response differs significantly beyond about 40°.

In general, weak VTI-type anisotropy of spherical waves causes more departure from the isotropic plane-wave response below 30° than isotropic spherical waves alone, with Classes 4 and 3/4 being the exceptions. Near the critical angle, however, the depth dependence of isotropic spherical waves is significant for Classes 1 and 2. All classes, except true Class 1, could benefit from spreading corrections below 30°, however the scale varies from class to class.

References:

Aki, K.T., and Richards, P.G., 1980, Quantitative Seismology: Theory and Methods: Vol. 1, W.H. Freeman and Co.

Castagna, J.P., Swan, H.W., and Foster, D.J., 1998, Framework for AVO gradient and intercept interpretation: Geophysics, **63**, 948-956.

Downton, J.E., and Lines, L.R., 2001, Constrained three parameter AVO inversion and uncertainty analysis: 71st Ann. Internat. SEG Mtg., Expanded Abstracts, 251-254.

Graebner, M., 1992, Plane-wave reflection and transmission coefficients for a transversely isotropic solid: Geophysics, **57**, 1512-1519.

Henneke, E.G., 1972, Reflection-refraction of a stress wave at a plane boundary between anisotropic media: J. Acoust. Soc. Am., **51**, 210-217.

Kelly, M.C., and Skidmore, C., 2001, Non-linear AVO equations and their use in 3-parameter inversions: 71st Ann. Internat. SEG Mtg., Expanded Abstracts, 255-256.

Krail, P.M., and Brysk, H., 1983, Reflection of spherical seismic waves in elastic layered media: Geophysics, **48**, 655-664.

Lavaud, B., Kabir, N., and Chavent, G., 1999, Pushing AVO inversion beyond linearized approximation: 61st Ann. Internat. EAGE Mtg., Expanded Abstracts, paper 6-49.

Roberts, G., 2000, Wide-Angle AVO: 70th Ann. Internat. Mtg., Soc. Expl. Geophys., Expanded Abstracts, 134-137.

Rueger, A., 1996, Reflection coefficients and azimuthal AVO analysis in anisotropic media: Ph.D. Thesis, Colorado School of Mines.

Rutherford, S.R., and Williams, R.H., 1989, Amplitude-versus-offset variations in gas sands: Geophysics, **54**, 680-688.

Skidmore, C., Cotton, R., and Kelly, M., 2001, AVO Rollover: A saturation sensitive direct hydrocarbon indicator: 71st Ann. Internat. SEG Mtg., Expanded Abstracts, 243-246.

Weyl, H., 1919, Ausbreitung elektromagnetischer Wellen ueber einem ebenen Leiter: Ann. Physik, **60**, 481-500.

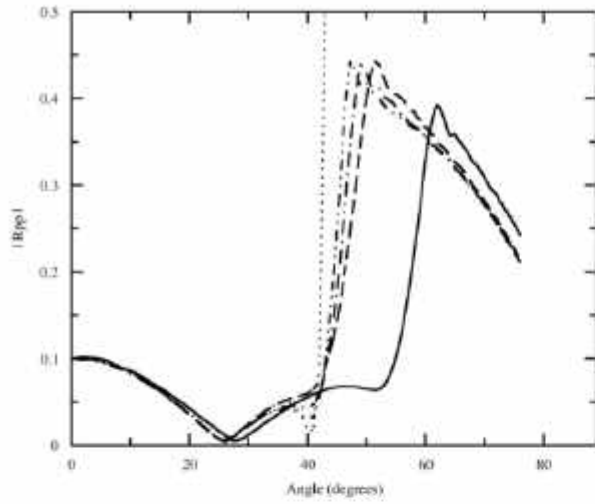**Fig. 1: AVO-Class 1 Spherical Wave PP Reflection Coefficients**

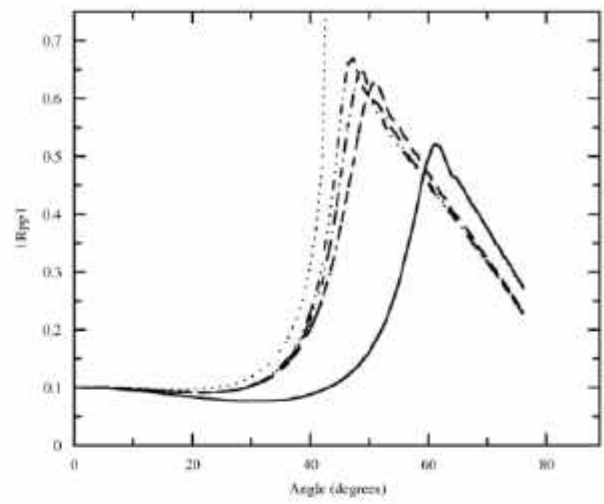**Fig. 2: AVO-Class 1f Spherical Wave PP Reflection Coefficients**

Fig. 3: AVO-Class 2 Spherical Wave PP Reflection Coefficients
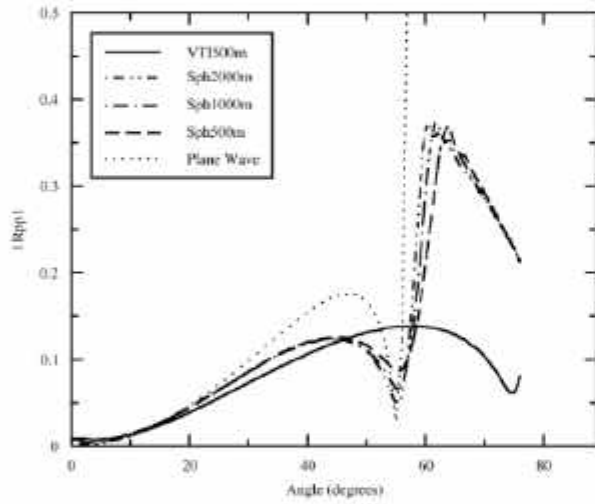
Fig. 4: AVO-Class 3 Spherical Wave PP Reflection Coefficients
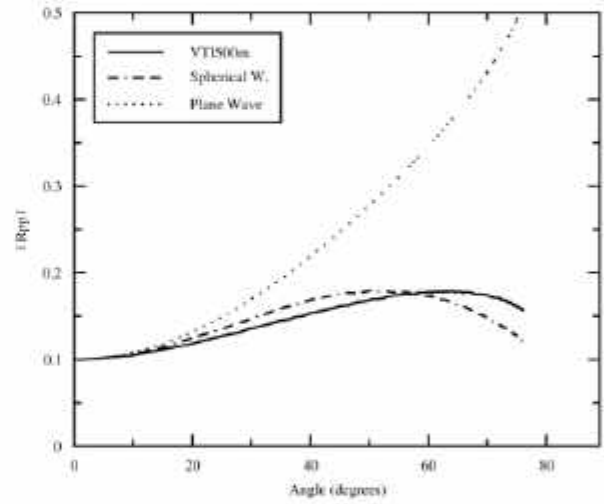
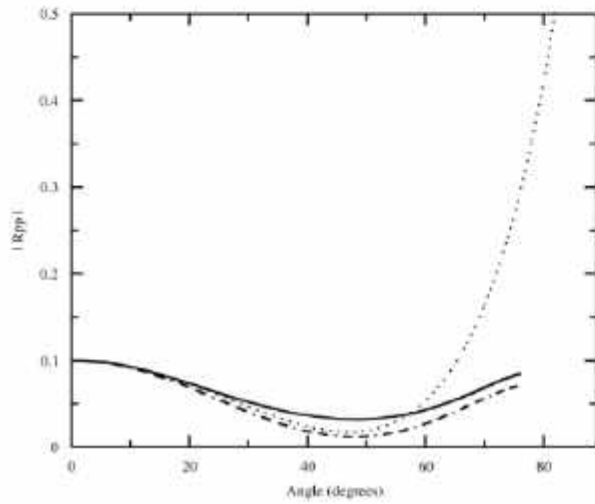**Fig. 5: AVO-Class 4 Spherical Wave PP Reflection Coefficients**

Fig. 6: AVO-Class 3/4 Spherical Wave PP Reflection Coefficients